

Contribution from the Department of Chemistry, Northeastern University, Boston, Massachusetts 02115, and the Francis Bitter National Magnet Laboratory, Massachusetts Institute of Technology, Cambridge, Massachusetts 02139

## High-Field Mössbauer Spectroscopy and Magnetization Studies of Linear-Chain Antiferromagnets. Field-Induced Paramagnetism of Hydrazinium Ferrous Sulfate

WILLIAM MICHAEL REIFF,<sup>1a</sup> HERBERT WONG,<sup>1a</sup> RICHARD B. FRANKEL,<sup>1b</sup> and SIMON FONER<sup>1b</sup>

Received August 30, 1976

AIC60633W

Isothermal Mössbauer and magnetic moment measurements have been made for powder samples of the linear-chain antiferromagnet  $\text{Fe}(\text{N}_2\text{H}_5)_2(\text{SO}_4)_2$  in magnetic fields up to  $\sim 150$  kG for  $T \leq 4.2$  K. The results indicate a transition from an antiferromagnetically ordered state to a paramagnetic state at a critical value of the applied field  $H_s$ , where  $75 \text{ kG} \leq H_s \leq 83 \text{ kG}$ . The onset of this behavior is clearly visible in the observation of additional transitions in the Mössbauer spectrum above  $H_s$ . Coincidentally, a rapid rise in moment with increasing field at  $H_0 \approx 75 \text{ kG}$  is observed although magnetic saturation is not reached even for  $H_0 = 150 \text{ kG}$  at 1.5 K. The intensity of the Mössbauer spectrum of the initial antiferromagnetic state approaches zero for  $H_0 \approx 125 \text{ kG}$  indicating essentially complete transformation to the paramagnetic state at these fields.

### I. Introduction

Antiferromagnetic systems in which the exchange interactions are quasi one dimensional, so-called linear-chain magnets, are interesting experimentally because their magnetic properties can be compared to exact theoretical predictions under certain circumstances. This class of magnetic systems is defined by a large ratio of the intrachain exchange  $J$  to the interchain  $J'$ ,  $|J/J'| \gg 1$  (taking the interaction between spins to be  $-2J\vec{S}_1 \cdot \vec{S}_2$ ).

In systems for which the intrachain exchange is ferromagnetic ( $J > 0$ ) and the interchain exchange is antiferromagnetic ( $J' < 0$ ), a magnetic field applied along the easy axis will, in general, induce one or more metamagnetic transitions to a paramagnetic state (Figure 1a), when  $\mu H_0 \geq J'$ . In systems for which  $J < 0$ , a magnetic field applied along the easy axis will induce a transition to a paramagnetic state when  $\mu H_0 \geq |J|$  (Figure 1b). Examples of the former case ( $J > 0$ ,  $J' < 0$ ) include  $\text{M}(\text{py})_2\text{Cl}_2$  ( $\text{M} = \text{Fe}, \text{Co}, \text{Ni}$ ),<sup>2,3</sup> whereas  $\text{Mn}(\text{py})_2\text{Cl}_2$ <sup>4</sup> and  $\text{Cu}(\text{py})_2\text{Cl}_2$ <sup>5</sup> are examples of the latter case ( $J < 0$ ).

The magnetization of an ideal antiferromagnetic linear chain of spins with  $S = 1/2$  has been calculated by Griffiths<sup>6</sup> and by Bonner and Fisher.<sup>7</sup> For Heisenberg exchange the results predict  $M$  and  $\partial M/\partial H_0$  to increase monotonically with increasing  $H_0$  until  $\partial M/\partial H$  approaches  $\infty$  and changes discontinuously at a critical value of the applied field. For Ising exchange,  $M$  changes discontinuously at a critical field. Matsuura<sup>8</sup> measured the high-field magnetization of  $\text{Cu}(\text{py})_2\text{Cl}_2$  but did not reach the transition field because of the relatively large intrachain exchange ( $|J/k| \approx 13.5$ ). For a spin  $1/2$  system such as the preceding Cu compound, the critical field is given by the expression

$$H_s = \frac{2(\gamma + 1)|J|}{g\beta}$$

where  $\gamma$  is a measure of the anisotropy of the exchange interaction with  $\gamma = 0$  the Ising case and  $\gamma = 1$  the Heisenberg case.

In this article we report the first spectroscopic observation of a magnetic field induced transition of a linear-chain antiferromagnet, in particular,  $\text{Fe}(\text{N}_2\text{H}_5)_2(\text{SO}_4)_2$ , hydrazinium ferrous sulfate. A schematic diagram for this compound is given in Figure 2. The system is a chain polymer with the individual ferrous ions in a distorted six-coordinate environment of four sulfate oxygen atoms and trans hydrazinium nitrogen atoms.<sup>9</sup> Recent powder susceptibility<sup>10</sup> and heat capacity<sup>11</sup> measurements show this compound to be a linear-chain antiferromagnet with  $T_N = 6.02 \text{ K}$ <sup>11</sup> characterized

by weak, negative intrachain (along the  $b$  axis via sulfate oxygen) exchange ( $J$ ) and even weaker interchain antiferromagnetic coupling ( $J'$ ), perhaps via hydrogen bonding. These results are summarized<sup>10</sup> as  $J'/J \approx 3 \times 10^{-2}$ ,  $J/K \approx -2$  to  $-3 \text{ K}$ , and a single-ion zero-field splitting parameter  $D \approx +2.5$ – $6 \text{ K}$ . The preceding ranges of parameters are the results of "best fits" of the temperature dependence of the molar susceptibility and magnetic heat capacity assuming a Heisenberg linear-chain model with  $S = 2$  and uniaxial single ion anisotropy. However the analysis of Wittveen and Reedijk<sup>10</sup> indicates that the character of the chain system is intermediate between the Heisenberg and Ising models. Since the entropy change at  $T_N$  for the present compound indicates  $S = 2$ ,<sup>11</sup> the Bonner-Fisher-Griffith model cannot be quantitatively applied. In addition the present measurements are for  $T < T_N$ , which is not considered in the preceding analyses. However, a crude estimate of the transition field  $H_s$  can be obtained from  $g\mu H_s \approx 2|J|S$ . Taking  $J/k = 2.5 \text{ K}$ <sup>10</sup> and assuming  $g = 2$  and  $S = 2$ ,  $H_s = 75 \text{ kG}$ . Below we present high-field magnetization and Mössbauer spectroscopy on powder samples of  $\text{Fe}(\text{N}_2\text{H}_5)_2(\text{SO}_4)_2$  from which we obtain a measure of  $H_s$ .

### II. Experimental Methods

The sample of  $\text{Fe}(\text{N}_2\text{H}_5)_2(\text{SO}_4)_2$  studied was obtained as a polycrystalline powder by methods described<sup>12</sup> in the literature and gave the required analytical results (Chemalytics Inc., Tempe, Ariz.). The purity of the sample was also confirmed by zero-field Mössbauer spectra at ambient temperature and 78 K with the pertinent parameters, quadrupole splitting ( $\Delta E_Q = 3.71 \text{ mm/s}$ ) and isomer shift ( $\delta_{\text{Fe}} = 1.29 \text{ mm/s}$ ) in accord with previously reported values.<sup>12</sup> The magnetization measurements to 150 kG were made with a low-frequency vibrating-sample magnetometer adapted to a water-cooled, high-field Bitter solenoid. Mössbauer spectra at 4.2 K in longitudinal external magnetic fields were obtained up to 83 kG using a superconducting magnet and up to 123 kG using a water-cooled Bitter solenoid. The effect of fringing fields from the Bitter solenoid was minimized by using a high intensity  $\gamma$ -ray source (120-mCi <sup>57</sup>Co on rhodium metal at 4.2 K) at a large source to detector distance. Vibrations of the solenoid from the passage of the cooling water resulted in some broadening of the spectra (Figure 6). The spectrum of Figure 4 was fit with the program of Stone.<sup>13</sup>

### III. Results

**Magnetization Measurements.** The magnetization data for the polycrystalline powders are shown in Figure 3. With increasing field at 4.2 K, below the three-dimensional ordering temperature of  $\sim 6 \text{ K}$ , one observes a monotonically increasing magnetic moment  $\sigma$  with the maximum value of  $\partial\sigma/\partial H$  occurring between 80 and 90 kG. At high fields,  $\partial\sigma/\partial H$  decreases but is not zero even at 150 kG. With decreasing field,

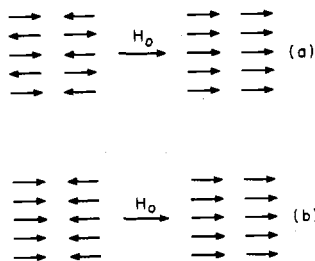


Figure 1. Magnetically induced phase transitions in linear-chain antiferromagnets with (a) negative intrachain exchange coupling and (b) positive intrachain exchange coupling.

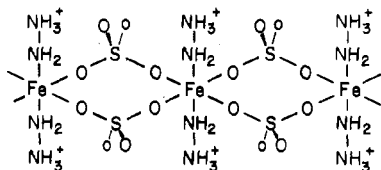


Figure 2. Schematic representation of linear-chain  $\text{Fe}(\text{N}_2\text{H}_5)_2(\text{SO}_4)_2$ .

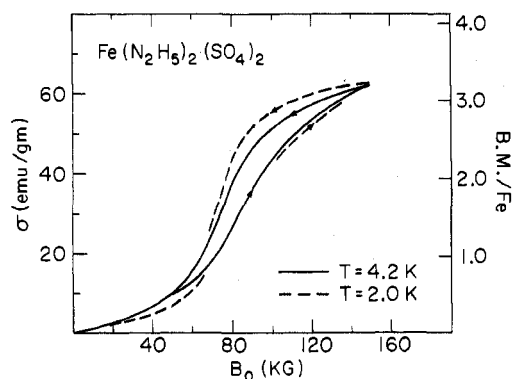


Figure 3. Isothermal magnetization of polycrystalline  $\text{Fe}(\text{N}_2\text{H}_5)_2(\text{SO}_4)_2$  vs. applied field for  $T = 2.0$  and  $4.2$  K.

hysteresis is observed, with the maximum in  $\partial\sigma/\partial H$  occurring at  $\sim 75$  kG. Below  $4.2$  K, the rapid rise in moment is more pronounced and the hysteresis is larger. The value of the moment at highest field corresponds to approximately  $3.7 \mu_B$ /iron atom, which is within 10% of the spin-only saturation (low temperature, high field) value,  $g\mu_B S$ , for the  $\text{Fe}^{2+}$  as a free ion ( $g = 2$ ,  $S = 2$ ).

In a powder sample one expects the critical field to be reached first in those crystallites which are fortuitously oriented such that the field is applied along the easy magnetic axis. For other orientations, the critical field corresponds to the projection of the applied field on the easy axis. We expect that for  $H_0$  aligned along the easy axis the largest value of  $\partial\sigma/\partial H$  occurs just below  $H_s$  and the moment is constant above  $H_s$ . For a polycrystalline material the character of the magnetic moment vs. field is expected to be broadened so that the value of  $H_s$  is less well defined. Including the observed hysteretic effects we obtain a range of  $H_s$  from the data given by  $75 \text{ kG} \lesssim H_s \lesssim 90 \text{ kG}$ .

The rapid change in magnetization to a value close to saturation, as well as the hysteresis, suggests a transition of first order, from the antiferromagnetic alignment to a paramagnetic phase. Although the hysteresis at  $2.0$  K is somewhat larger than at  $4.2$  K, the transition field is approximately the same. A relatively temperature-independent transition field and hysteresis are reminiscent of metamagnetic transitions in ordered systems.

**Mössbauer Measurements.** The temperature dependence of the zero-field Mössbauer spectrum has been studied below  $6$  K and consists of a sharp Zeeman pattern. This result is

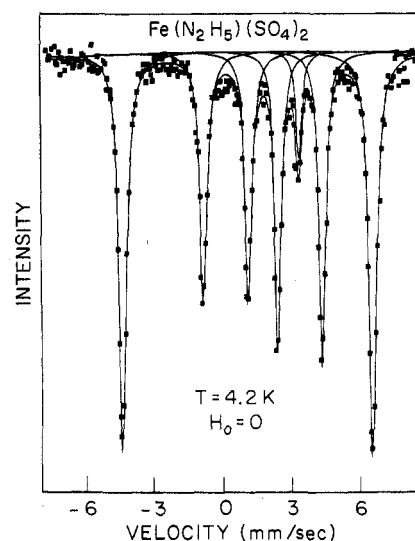
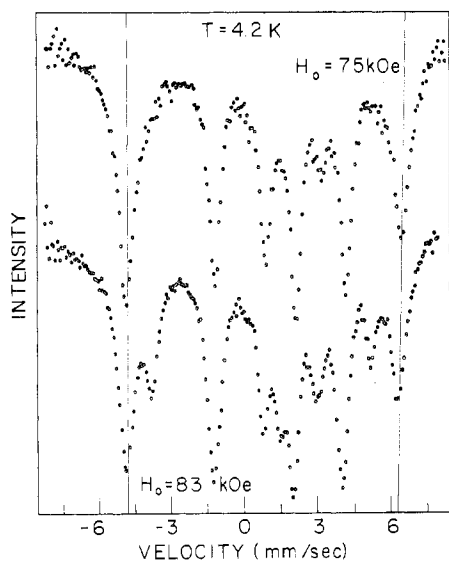


Figure 4. Mössbauer spectrum of polycrystalline  $\text{Fe}(\text{N}_2\text{H}_5)_2(\text{SO}_4)_2$  at  $4.2$  K,  $H = 0$ . The continuous curve is a computer fit assuming Lorentzian line shapes.

consistent with the previous observation<sup>11</sup> of a sharp  $\lambda$ -like anomaly in the magnetic heat capacity at  $6.02 \pm 0.05$  K along with a distinct broad maximum centered at  $\sim 12$  K where the latter is associated with the one-dimensional intrachain antiferromagnetic interactions of the system. An interesting feature is that the zero-field Mössbauer spectra exhibit a gradual broadening-hyperfine splitting process over the range  $15$ – $6$  K. This may also reflect one-dimensional behavior of the system or may be ascribed to relaxation effects. Above  $15$  K, the spectrum consists of a sharp quadrupole doublet.

A determination of the sign of the principal component of the electric field gradient tensor  $V_{zz}$  has been made by observing the Mössbauer spectrum in an external magnetic field at  $77$  K. The spectrum consists of the doublet-triplet of a rapidly relaxing paramagnet with the apparent triplet at lower energy. This implies that the sign of  $V_{zz}$  is positive (i.e., the  $M = \pm 3/2$  nuclear sublevels lie above the  $M = \pm 1/2$  levels). The triplet-doublet form of the spectrum also indicates the asymmetry parameter  $\eta$  is small (ca.  $\leq 0.3$ ).  $\text{Fe}(\text{N}_2\text{H}_5)_2(\text{SO}_4)_2$  is known<sup>9</sup> to be isomorphous to  $\text{Zn}(\text{N}_2\text{H}_5)_2(\text{SO}_4)_2$  for which the x-ray structure data indicate a tetragonal compression of the local coordination environment. For iron(II), stronger axial ligation usually results in destabilization of the  $d_{xz}$  and  $d_{yz}$  orbitals (for negligible axial  $\pi$  delocalization) to give a ground  $d_{xy}$  orbital corresponding to a  ${}^5B_2$  ground term in the absence of spin-orbit coupling, i.e., an axial ligand field component  $\Delta > \lambda$ . In this situation a large, positive quadrupole effect is expected and accords with our magnetically perturbed spectrum at  $77$  K. The foregoing ground state is also suggested from fits<sup>12</sup> to the temperature dependence of the quadrupole splitting and magnetic moment over the temperature range  $300$ – $78$  K. The analysis is consistent with an orbital singlet ground term and axial field  $\Delta \approx 10\lambda$ , where  $\lambda_0 = -100 \text{ cm}^{-1}$  for  $\text{Fe}^{2+}$ .

Using the preceding result that  $V_{zz}$  is positive and  $\eta < 0.3$  and taking the magnitude of  $H_{\text{hf}}$  from the lines of the  $4.2$  K,  $H_0 = 0$  spectrum corresponding to the ground-state splitting, a reasonable representation of the spectrum of Figure 4 is obtained with the parameters  $H_{\text{hf}} = -260$  kG,  $\Delta E = +3.70$  mm/s,  $\eta = 0.3$ , and the angle between  $V_{zz}$  and  $H_{\text{hf}}$ ,  $\beta \approx 65^\circ$ , by comparison of the observed spectrum with computer simulations using a program by Singh and Hoy.<sup>14</sup> Assuming that the axis of  $V_{zz}$  coincides with the trans N–Fe–N direction, the preceding fit suggests that the spins of this system are tipped away from the N–Fe–N direction toward the  $b$ – $c$  plane,



**Figure 5.** Mössbauer spectra of polycrystalline  $\text{Fe}(\text{N}_2\text{H}_5)_2(\text{SO}_4)_2$  vs. longitudinal field for  $T = 4.2$  K and  $H_0 = 75$  and  $83$  kOe.

which is that defined by the bridging sulfate oxygens of the chemical linear chain.

The effect of a longitudinally applied magnetic field on the Mössbauer spectrum at 4.2 K is shown in Figures 5 and 6. For  $H_0 < 75$  kG, the effect of the applied field is simply to increase the line width compared with  $H_0 = 0$  because the total field at each nuclear site is the vector sum of the applied field and the hyperfine field arising from the alignment of the electron spin by the antiferromagnetic exchange interaction. At slightly higher fields, one observes (Figure 5) the discontinuous appearance of new lines, called spectrum B, in addition to the lines of spectrum A. As the external field is further increased (Figure 6), spectrum B increases and spectrum A decreases in intensity, until at 123 kG spectrum A has vanished and only spectrum B is observed. One of the chief characteristics of spectrum A is that the line position is nearly independent of field, and the effect of the applied field is to broaden the lines. This is the usual behavior for an antiferromagnet in powder form. In spectrum B, the line position in an external magnetic field is field dependent, with the overall splitting decreasing with increasing applied field.

The foregoing results can be understood if one assumes that, in a given applied field, spectrum A corresponds to crystallites in the powder sample in which the spins are antiferromagnetically aligned, while spectrum B corresponds to crystallites in which the spins have undergone a transition to a paramagnetically aligned configuration and are polarized in the direction of  $H_0$ . The field at which the transition occurs in each crystallite depends on its initial crystallographic orientation with respect to the applied field. Presumably, as discussed above in connection with the magnetization measurements, the transition occurs initially in those crystallites which are fortuitously aligned with the magnetic easy axis parallel to the external field. Transitions in the other crystallites would be induced when the applied field is large enough so that its projection on the easy axis or another of the principal magnetic axes exceeds the minimum value for that axis. Because of the magnetocrystalline anisotropy, the spins in the crystallites in the new paramagnetic phase are not aligned strictly parallel to the applied field. This is indicated by the fact that the susceptibility of the powder is still increasing even at 150 kG. The spectra in Figure 5 show that the AF  $\rightarrow$  P transition at 4.2 K occurs between 75 and 83 kG for  $H_0$  along the easy axis. The AF  $\rightarrow$  P process is essentially complete for the random powder sample in a field  $\sim 125$  kG.

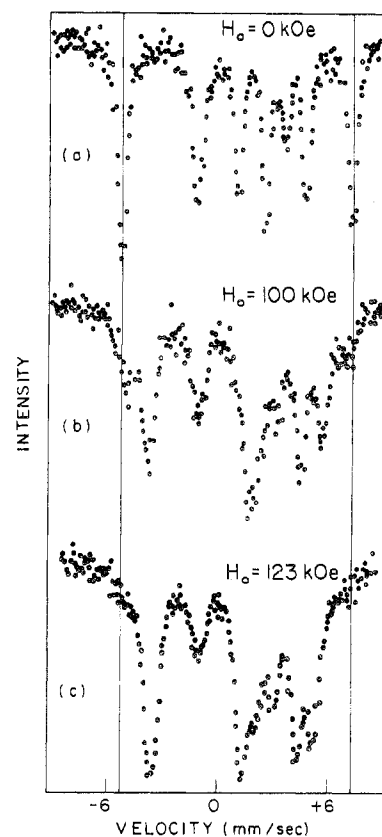


**Figure 6.** Mössbauer spectra of polycrystalline  $\text{Fe}(\text{N}_2\text{H}_5)_2(\text{SO}_4)_2$  vs. longitudinal field for  $T = 4.2$  K and (a)  $H = 0$  kOe, (b)  $H = 100$  kOe, and (c)  $H = 123$  kOe.

The spectrum in the antiferromagnetic phase (spectrum A) is unshifted by the applied field, but the lines are broadened. The spectrum of the paramagnetic phase is shifted to lower field, which indicates that the sign of the magnetic hyperfine interaction is negative. Because the spins in the paramagnetic phase tend to orient along the applied field, the angle  $\beta$  between the net magnetic field at the nucleus and the principal component of the electric field gradient tensor  $V_{zz}$  becomes randomized in the powder sample, giving the complicated spectrum observed at higher field (Figure 6). In addition, anisotropy of the hyperfine interaction itself further complicates this spectrum.

These results in Figure 5 show that  $75 \text{ kG} \leq H_s \leq 83 \text{ kG}$  for  $\text{Fe}(\text{N}_2\text{H}_5)_2(\text{SO}_4)_2$  at 4.2 K and correlate well with the rapid rise observed in the magnetization measurements. They also illustrate the effectiveness of Mössbauer spectroscopy in observing the microscopic behavior of these transitions, even in powder samples. In order to elucidate the nature of the transition in more detail, single-crystal measurements are necessary.

**Acknowledgment.** W.M.R. acknowledges the support of the National Science Foundation, Division of Materials Research, Solid State Chemistry Program (Grant No. DMR 75-13592A01). He also acknowledges the partial support of the Research Corp. and HEW Grant No. RR 07143. The Francis Bitter National Magnet Laboratory is supported by the National Science Foundation. We wish to thank E. J. McNiff, Jr., for assistance with the high-field magnetic measurements.

**Registry No.**  $\text{Fe}(\text{N}_2\text{H}_5)_2(\text{SO}_4)_2$  (salt form), 53091-69-3;  $\text{Fe}(\text{N}_2\text{H}_5)_2(\text{SO}_4)_2$  (complex form), 61689-47-2.

#### References and Notes

- (1) (a) Northeastern University. (b) Massachusetts Institute of Technology.
- (2) (a) S. Foner, R. B. Frankel, W. M. Reiff, B. F. Little, and G. J. Long,

- Solid State Commun.*, **16**, 159 (1975); (b) S. Foner, R. B. Frankel, E. J. McNiff, W. M. Reiff, B. F. Little, and G. J. Long, *AIP Conf. Proc.*, No. **24**, 363 (1974).
- (3) S. Foner, R. B. Frankel, W. M. Reiff, H. Wong, and G. Long, *AIP Conf. Proc.*, No. **25**, (1975).
- (4) P. M. Richards, R. K. Quinn, and B. Moricin, *J. Chem. Phys.*, **59**, 4474 (1973).
- (5) K. Takeda, S. Matsukowa, and T. Haseda, *J. Phys. Soc. Jpn.*, **30**, 1330 (1971).
- (6) R. B. Griffiths, *Phys. Rev. [Sect.] A*, **133**, 768 (1964).

- (7) J. C. Bonner and M. E. Fisher, *Phys. Rev. [Sect.] A*, **135**, 640 (1964).
- (8) M. Matsuura, *Phys. Lett. A*, **34**, 274 (1971).
- (9) C. K. Prout and H. M. Powell, *J. Chem. Soc.*, 4177 (1961).
- (10) H. T. Witteveen and J. Reedijk, *J. Solid State Chem.*, **10**, 151 (1974).
- (11) F. W. Klaaijzen, H. Den Adel, Z. Dakouil, and W. J. Huiskamp, *Physica B (Amsterdam)*, **79B + C**, 113 (1975).
- (12) A. Nieuwpoort and J. Reedijk, *Inorg. Chim. Acta*, **7**, 323 (1973).
- (13) G. M. Bancroft, A. G. Maddock, W. K. Ong, R. H. Prince, and A. J. Stone, *J. Chem. Soc. A*, 1966 (1967).
- (14) K. P. Singh and G. R. Hoy, private communication.

Contribution from Department of Chemistry,  
University of Idaho, Moscow, Idaho

## Trifluoromethanesulfinate Esters

CRAIG A. BURTON and JEAN'NE M. SHREEVE\*

Received December 29, 1976

AIC60925X

An improved route to the synthesis of trifluoromethanesulfinyl chloride by oxidation of trifluoromethanesulfonyl chloride with *m*-chloroperbenzoic acid is reported. Additional study of the metathetical reactions of  $\text{CF}_3\text{S}(\text{O})\text{X}$  ( $\text{X} = \text{F}, \text{Cl}$ ) has resulted in the preparation of the new compounds  $\text{CF}_3\text{S}(\text{O})\text{CN}$ ,  $[\text{CF}_3\text{S}(\text{O})\text{OCH}_2]_2$ ,  $[\text{CF}_3\text{S}(\text{O})\text{OCH}_2]_2\text{CHOH}$ ,  $\text{CF}_3\text{S}(\text{O})\text{ON}(\text{CF}_3)_2$ , and  $\text{CF}_3\text{S}(\text{O})\text{CH}_2\text{C}(\text{O})\text{CH}_3$ . With ethylene oxide,  $\text{CF}_3\text{S}(\text{O})\text{Cl}$  gives  $\text{CF}_3\text{S}(\text{O})\text{OCH}_2\text{CH}_2\text{Cl}$ .

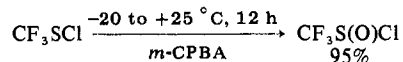
### Introduction

Trifluoromethanesulfinyl chloride and trifluoromethanesulfinyl fluoride are useful reagents for introducing the trifluoromethanesulfinyl group into a variety of compounds by reaction with alcohols,<sup>1</sup> amines,<sup>1</sup> and lithium salts.<sup>2</sup> For use in these reactions, the trifluoromethanesulfinyl fluoride was obtained from a multistep process involving fluorination of bis(trifluoromethyl)disulfane with  $\text{AgF}_2$  to form  $\text{CF}_3\text{SF}_3$  which was hydrolyzed subsequently by catalytic amounts of water in a Pyrex glass vessel<sup>3</sup>.



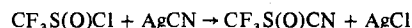
Further reaction of  $\text{CF}_3\text{S}(\text{O})\text{F}$  with anhydrous hydrogen chloride produced  $\text{CF}_3\text{S}(\text{O})\text{Cl}$  in nearly quantitative yields.<sup>4</sup>

We now find that  $\text{CF}_3\text{S}(\text{O})\text{Cl}$  results from the oxidation of  $\text{CF}_3\text{SCl}$  which is a less expensive and more readily accessible precursor than the disulfane



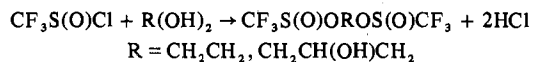
Fluorination of  $\text{CF}_3\text{S}(\text{O})\text{Cl}$  with  $\text{NaF}$  gives  $\text{CF}_3\text{S}(\text{O})\text{F}$  essentially quantitatively.<sup>4</sup>

A large number of compounds have resulted from the reactions of trifluoroacetyl chlorides or bromides with silver pseudohalides. It has been shown that a similar reaction occurs between trifluoromethanesulfinyl chloride and silver isocyanate to form  $\text{CF}_3\text{S}(\text{O})\text{NCO}$ .<sup>5</sup> We now find that the analogous reaction occurs with silver cyanide<sup>6</sup>

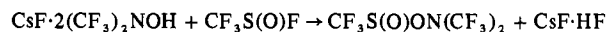
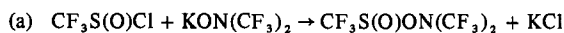


However, this reaction mode does not extend to the preparation of  $\text{CF}_3\text{S}(\text{O})\text{SCN}$ .

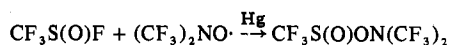
Reaction of trifluoromethanesulfinyl halides has also been found to occur with compounds containing labile hydrogens, such as alcohols, to form trifluoromethanesulfinate esters.<sup>1</sup> Such reactions have now been carried out with di- and triols to give bis(trifluoromethanesulfinyl) compounds which comprise the first members of a new class



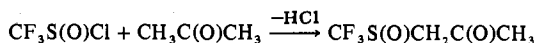
Previously, it was shown that trifluoromethanesulfinyl bis(trifluoromethyl)nitroxide,  $\text{CF}_3\text{S}(\text{O})\text{ON}(\text{CF}_3)_2$ , could be prepared by two routes<sup>7</sup>



In this work, another route to this sulfinyl ester was attempted in order to learn more about the fluorine atom abstracting ability of the stable radical  $(\text{CF}_3)_2\text{NO}^\bullet$ , in the presence of mercury.<sup>8</sup> It was found that this reaction proceeds easily with  $\text{CF}_3\text{S}(\text{O})\text{F}$  and trifluoromethanesulfinyl bis(trifluoromethyl)nitroxide results<sup>6</sup>

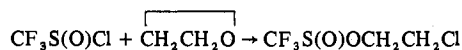


In a reaction reported earlier by others,<sup>9</sup> trifluoromethanesulfonyl chloride was reacted with acetone to give  $\text{CF}_3\text{SCH}_2\text{C}(\text{O})\text{CH}_3$ . We find that the reaction with trifluoromethanesulfinyl chloride occurs similarly to yield  $\text{CF}_3\text{S}(\text{O})\text{CH}_2\text{C}(\text{O})\text{CH}_3$



This new compound is similar to acetylacetone and preliminary work indicates that it may act as a bidentate ligand with appropriate metals.

In addition, we have found that trifluoromethanesulfinyl chloride reacts with ethylene oxide to yield the corresponding chloro ester in good yield



### Results and Discussion

The improved synthesis of trifluoromethanesulfinyl chloride by oxidation of trifluoromethanesulfonyl chloride with *m*-chloroperbenzoic acid has several advantages in comparison with the previously reported method. In the earlier method, it is necessary to prepare  $\text{AgF}_2$  by high-temperature fluorination of  $\text{AgF}$  with elemental fluorine. Also, the reaction sequence requires the use of bis(trifluoromethyl)disulfane